

Adenosine-Deaminase-Acting-on-RNA-1 Facilitates T-cell Migration toward Human Melanoma Cells

Naama Margolis^{1,2}, Hanna Moalem^{1,2}, Tomer Meirson^{1,3}, Gilli Galore-Haskel^{1,4}, Ettai Markovits^{1,2}, Erez N. Baruch^{1,2}, Bella Vizek^{1,2}, Avner Yeffet⁵, Julia Kanterman-Rifman⁵, Assaf Debby^{6,7}, Michal J. Besser^{1,2}, Jacob Schachter¹, and Gal Markel^{1,2,3}



ABSTRACT

The effect of tumor/T-cell interactions on subsequent immune infiltration is undefined. Here, we report that preexposure of melanoma cells to cognate T cells enhanced the chemotaxis of new T cells *in vitro*. The effect was HLA class I-restricted and IFN γ -dependent, as it was abolished by β 2M-knockdown, MHC-blocking antibodies, JAK1 inhibitors, JAK1-silencing and IFN γ R1-blocking antibodies. RNA sequencing (RNA-seq) of 73 melanoma metastases showed a significant correlation between the interferon-inducible p150 isoform of adenosine-deaminase-acting-on-RNA-1 (ADAR1) enzyme and immune infiltration. Consistent with this, cocultures of cognate melanoma/T-cell pairs led to IFN γ -dependent induction of ADAR1-p150 in the melanoma cells, as visualized *in situ* using dynamic cell blocks, *in ovo* using fertilized chick eggs, and *in vitro* with Western blots. ADAR1 staining and RNA-seq in patient-

derived biopsies following immunotherapy showed a rise in ADAR1-p150 expression concurrently with CD8⁺ cell infiltration and clinical response. Silencing ADAR1-p150 abolished the IFN γ -driven enhanced T-cell migration, confirming its mechanistic role. Silencing and overexpression of the constitutive isoform of ADAR1, ADAR1-p110, decreased and increased T-cell migration, respectively. Chemokine arrays showed that ADAR1 controls the secretion of multiple chemokines from melanoma cells, probably through microRNA-mediated regulation. Chemokine receptor blockade eliminated the IFN γ -driven T-cell chemotaxis. We propose that the constitutive ADAR1 downregulation observed in melanoma contributes to immune exclusion, whereas antigen-specific T cells induce ADAR1-p150 by releasing IFN γ , which can drive T-cell infiltration.

Introduction

The presence of T cells at the tumor margin correlates both with response to immunotherapy and T-cell infiltration (1). The factors that increase the chemotactic potential of tumor cells to allow immune infiltration remain unknown. T cells interact with tumor cells through their T-cell receptor, which binds peptide-MHC complexes (2, 3). The interaction between T cells and tumor cells can cause the T cells to secrete IFN γ , thus activating the IFN γ pathway in tumor cells (4).

The IFN γ signaling pathway begins with binding of IFN γ to the IFN γ receptor (IFN γ R), which is comprised of two subunits IFN γ R1 and IFN γ R2. These subunits then oligomerize and transphosphorylate, activating JAK1 and JAK2 (5). JAK1 and JAK2 phosphorylate STAT1. Phosphorylation of STAT1 enables the formation of STAT1 homodimers that translocate into the nucleus and bind to the promoters of target genes (5) causing induction of many interferon-stimulated genes (ISG; ref. 6).

Tumor-infiltrating lymphocytes (TIL) have express high levels of the chemokine receptors CXCR3, CCR5, and CCR4 (7), suggesting that the

ligands for these receptors could play a part in T-cell infiltration of tumors. The chemokines CXCL9, CXCL10, and CXCL11 are all induced by IFN γ and are the ligands for CXCR3 (8), making them likely candidates for raising the chemotactic potential of tumor cells.

Adenosine-deaminase-acting-on-RNA-1 (ADAR1) is an RNA editing enzyme that converts adenosine into inosine. ADAR1 has two isoforms, one is interferon-induced (p150) and one is transcribed constitutively (p110; ref. 9). ADAR1 affects the expression of many genes either through editing in coding regions or in noncoding regions, which can alter RNA stabilization, splicing and nuclear retention (10–12). In addition, ADAR1 edits noncoding RNAs, affecting their biogenesis and targets (13, 14). ADAR1 is downregulated during the metastatic transition of melanoma (15). This downregulation renders melanoma cells more tumorigenic and more immune resistant (15, 16).

Here, we report that ADAR1 influences T-cell infiltration of melanomas in two ways. On the one hand, downregulation of constitutive ADAR1-p110 during the metastatic transition reduces the chemotactic potential of melanoma cells and promotes immune exclusion. On the other hand, T-cell/melanoma interactions induce ADAR1-p150 expression, which causes an influx in TILs.

Methods

Patient consent

All human specimens were obtained following written informed consent and the studies were conducted in accordance with the Declaration of Helsinki, the Sheba Medical Center Institutional Review Board and Israel Ministry of Health. The melanoma cell lines and TIL cultures used in the current article were obtained as part of a clinical trial with adoptive transfer of TILs (Israel Ministry of Health Approval no. 3518/2004, clinicaltrials.gov Identifier NCT00287131). The tissue biopsies used in the current article were obtained either

¹Ella Lemelbaum Institute for Immuno-Oncology and Melanoma, Sheba Medical Center, Ramat Gan, Israel. ²Department of Clinical Microbiology and Immunology, Sackler Faculty of Medicine, Tel Aviv University, Tel Aviv-Yafo, Israel. ³Davidoff Cancer Center, Rabin Medical Center, Petah Tikva, Israel. ⁴4C Biomed Industries Ltd., Netanya, Israel. ⁵Innovo Mimetics Ltd., Jerusalem, Israel. ⁶Sackler Faculty of Medicine, Tel Aviv University, Tel Aviv-Yafo, Israel. ⁷Institute of Pathology, Sheba Medical Center, Ramat Gan, Israel.

Corresponding Author: Gal Markel, Davidoff Cancer Center, Rabin Medical Center, Petah Tikva 49504, Israel. Phone: 972-3937-7990; Fax: 972-3937-7902; E-mail: markel@tauex.tau.ac.il

Cancer Immunol Res 2022;10:1127–40

doi: 10.1158/2326-6066.CIR-21-0643

©2022 American Association for Cancer Research

from three different studies: TIL-treated patients, which is the same abovementioned TIL clinical trial; Fecal Microbial Transplantation plus Nivolumab in patients with refractory melanoma (Israel Ministry of Health Approval no. SMC-17/3956, clinicaltrials.gov Identifier NCT03353402); and from retrospective tissue collection of patients treated with anti-PD-1 as part of the real world melanoma clinic (Sheba Medical Center Approval SMC-2015/2411). The results of the TIL trial have been published (17, 18), the results of the Fecal Microbial Transplantation trial were published in 2021 (19), and the specimens from the real world melanoma clinic were described in a previous study (20). The full description of these trials, including inclusion and exclusion criteria of patients, how many patients were recruited and which types of biomaterials were collected, are fully available in these references. Tissue samples were collected through needle or surgical biopsies and were either fixed in paraffin-embedded blocks or used for melanoma and TIL culture development as described herein.

Cells and media

Melanoma cell lines 624mel (RRID:CVCL_8054) and 526mel (RRID:CVCL_8051) were obtained in 2005 from Dr. Steve Rosenberg (NCI, Bethesda, MD). mel014 was obtained from a patient with stable IV melanoma at our institute in 2010, as described previously (21). All three cell lines were maintained in RPMI1640 (01-100-1A, Biological Industries) supplemented with 10% FBS (04-127-1A, Biological Industries). After modification for CCL4 overexpression, ADAR1 overexpression, or ADAR1 knockdown (see **Expression constructs and stable transfections**) the cell lines were cultured in RPMI1640 supplemented with 10% FBS and either 1 µg/mL Puromycin (P001-100, Calbiochem) or 3 mg/mL G418 (ALX-380013, Enzo Life Sciences). Cells were used for periods of time of 1 to 2 months after thawing.

The TIL cell lines TIL014 and TIL096 were obtained from patients with stable IV malignant melanoma at our institute in 2010 as described previously (21). The TIL cell lines were maintained in RPMI1640 supplemented with 10% FBS and 3,000 IU/mL recombinant human IL2 (rhIL2; 3000014936, Novartis). Cells are used in line with approvals from the Sheba Medical Center Institutional Review Board and Israel Ministry of Health (Approval no. 3518/2004, clinicaltrials.gov Identifier NCT00287131). All cell lines were tested monthly for *Mycoplasma* using Hy-Mycoplasma Kit (KI50341, Hylabs).

Expression constructs and stable transfections

The ADAR1 knockdown system is based on shRNA oligonucleotides subcloned into pSuper.puro vector (VEC-PBS-0008, Oligoengine). The ADAR1-p110 overexpression construct was subcloned into pQCXIP vector (631516, Clontech). The mutation in the ADAR-p110 catalytic domain was introduced on the ADAR1-p110 overexpression construct and verified as previously described (15). The CCL4 overexpression construct was subcloned into pQCXIN vector (631514, Clontech). Primers used for the generation of all constructs appear below. Transfections were performed using Turbofect (R0531 Fermentas, Canada) according to the manufacturer's instructions. All three melanoma cell lines (mel526, mel624, and mel014) were transfected with all three constructs. Retroviral transduction of 293T cells was performed as previously described (22). All transfectants were routinely tested for expression.

Primers used:

ADAR1 knockdown: fw – GATCCCCGTTGACTAAGTCACATGTAAATTCAAGAGATTT ACATGTGACTTAGTCAACTTTTAA;

rev – AGCTTAAAAAGTTGACTAAGTCACATGTA AATCTCT-TGAATTTACATGTGACTTAGTCAACGGG

ADAR1-p110: fw – GGCAGCCTCCGGGTG; rev – CTGTCTGTG-CTCATAGCCTTGA

CCL4: fw – ATGAAGCTCTGCGTGACTG; rev – AGAAGCA-TCCGGGCTCAG

CRISPR

ADAR1-p150

500,000 melanoma cells were plated in a 10-cm plate and incubated at 37°C, 5% CO₂ overnight. Transfection mix was generated by mixing Edit-R All-in-one Lentiviral sgRNA (Custom-RNA, Dharmacon) targeting the start codon of the ADAR1 gene (DNA Target: 5' GAATCCGCGGCAGGTAAGCC 3' Organism: Gene ID: 103 Gene Symbol: ADAR Genomic Location: chr1:154608003-154607980 (-) Variant Targeted: NM_001111.4) and DharmaFECT1 transfection reagent (T-2001-02, Dharmacon) and incubated for 20 minutes at room temperature. The medium was then removed from the melanoma cells and replaced with the transfection mix. The plates were incubated at 37°C, 5% CO₂ for 72 hours. The transfection mix was then replaced with regular growth medium containing 1 µg/mL Puromycin for cell selection. Plates were incubated at 37°C, 5% CO₂ for 2 weeks. The level of expression of ADAR1-p150 was checked by Western blotting (see *Western blotting*).

β2M

500,000 melanoma cells were plated in a 10 cm plate and incubated at 37°C, 5% CO₂ overnight. Transfection mix included synthetic crRNA against exon-1 of the B2M gene (CM-004366-01, Dharmacon, target sequence: GAGTAGCGCGAGCACAGCTA, exon 1 NM_004048.2), tracrRNA (U-002005-05, Dharmacon), Cas9 nuclease protein (CAS11201, Dharmacon) and DharmaFECT1 transfection reagent and incubated for 20 min. The medium in which the melanoma cells were cultured was replaced with the transfection mix and plates were incubated at 37°C, 5% CO₂ for 14 to 18 hours. The transfection mix was then replaced with regular growth medium. Plates were incubated at 37°C, 5% CO₂ for 48 hours, until expression of β2M was assessed by flow cytometry.

Transient transfection

Either siRNA oligos targeting B2M (ON-TARGETplus Human B2M (567) siRNA – SMARTpool, L-004366-00-0010, Dharmacon), JAK1 (ON-TARGETplus Human JAK1 (3716) siRNA – SMARTpool, L-003145-00-0010, Dharmacon), or negative control oligos (ON-TARGETplus Non-targeting Pool, D-001810-10, Dharmacon) were used to transiently transfect melanoma cells with 10 nmol/L siRNA using JetPrime (114-15, Polyplus) according to the manufacturer's instructions. β2M expression was silenced in mel526 and mel014, and JAK1 expression was silenced in mel526 and mel624. 72 h post transfection, JAK1 expression was validated using western blot and β2M expression was validated using flow cytometry.

Chemotaxis assay

80,000 melanoma cells were seeded in flat 96-well plates for 24 hours at 37°C, 5% CO₂. TILs were stained using Calcein-AM (C1430, Invitrogen) according to the manufacturer's instructions. 40,000 stained TILs were seeded in the transwell insert containing 5-µm pores in a polycarbonate membrane (CLS3387, Corning). TILs were allowed to migrate for 4 hours at 37°C, 5% CO₂. The transwell inserts were removed and the TILs in the lower well were detached from the melanoma cells by adding EDTA 0.5M (01-862-1B, Biological

Industries) to a final concentration of 10 mmol/L and incubating at room temperature for 10 minutes. The TILs were then collected by thorough pipetting and counted using flow cytometry. Results are presented as percent over relative migration, a value that represents the delta in fold migration toward a specific target over nonspecific migration toward control. The absolute number of TILs migrated are available in the Supplementary Table S1.

Prior to the chemotaxis assay either the TILs or the melanoma cells were treated as indicated in each experiment using one for the following:

Neutralizing antibodies

Melanoma cells were incubated for 30 minutes on ice with either IFN γ -specific antibody 2 μ g/mL (ab134070 Abcam) and isotype control (IC; Rabbit IgG, monoclonal, ab172730, Abcam) or MHC class I-specific antibody 15 μ g/mL (w6/32, MABN1783, Mercury Millipore) and IC (Mouse IgG2a monoclonal, ab18415, Abcam). Following incubation TILs were added at an E:T ratio of 1:1 for 24 hours at 37°C, 5% CO₂. Following incubation, the medium was collected and IFN γ levels were quantified via ELISA (as detailed below). The melanoma cells were washed and seeded for the chemotaxis assay.

Inhibitors and antagonists

Melanoma cells were incubated with ruxolitinib (S1378, Selleckchem) 30 μ g/mL. TILs were incubated with a mix of three chemokine receptor antagonists Maraviroc (R&D) 5 μ mol/L, C021 (R&D) 0.3 μ mol/L, and AMG-487 (R&D) 0.5 μ mol/L for 1 hour at 37°C, 5% CO₂ prior to participating in the chemotaxis assay.

Recombinant proteins

IFN γ (R&D) 10 ng/mL was added to the culture medium of 1,000,000 melanoma cells seeded in a 10-cm plate and incubated for 24 hours at 37°C, 5% CO₂. Melanoma cells were then washed and reseeded for the chemotaxis assay. CCL5 (R&D) 100 ng/mL was added to melanoma cells culture medium just prior to participating in the chemotaxis assay.

Staining of the immune coculture cell microarray

Construction of the immune coculture cell microarray (ICCM) was performed as described previously (23). The ICCM block was sectioned to 4.5- μ m slides. Prior to immunofluorescence staining, slides were heated for 2 hours at 37°C, 5% CO₂. Deparaffinization was performed using xylene and ethanol, and slides were washed with PBST (PBS with 0.05% Tween-20). Antigen retrieval was conducted using immersion of slides in Citrate buffer (pH 6.0; C9999, Merck) and microwave heating. After cooldown, slides were washed and incubated for 1 hour at room temperature with a blocking solution containing 3% BSA (A7906, Merck). Slides were then washed and incubated overnight at 4°C with 200 μ L mix of primary antibodies against ADAR1 (Sigma-Aldrich catalog no. HPA003890, RRID:AB_1078103) and HMB-45 (Abcam catalog no. ab733, RRID:AB_305854) in 2% BSA or 2% BSA only for control. The following day, slides were washed and incubated with 200 μ L mix of secondary antibodies (donkey anti-rabbit -Alexa fluor 488 nm, 1:200, ab150065, Abcam; and donkey anti-mouse -Alexa fluor 594 nm, 1:200, ab150112, Abcam) for 1 hour at room temperature. Post-incubation, slides were washed, and DAPI stain was added (Hoechst stain in PBS, 1:2,000, H6024, Sigma-Aldrich). Slides were washed, and coverslips were glued using Fluoromount Aqueous Mounting fluid (F4680, Sigma-Aldrich). Images were acquired using the confocal microscope Leica TCS SP5 (Leica Biosystems). After filtration for background staining using

slides stained with secondary-only antibodies, no further filtration or change of microscope setting was done throughout the image capture process. Images were export into TIFF files using the Fiji software18 (version 1.51 W), with no change of filters.

Chick egg tumor xenograft model (*in ovo*) for testing human tumor cell/immune effector cell interactions

Melanoma cells were stained with Vybrant DiD (V22887, Thermo Scientific, MA) according to the manufacturer's instructions. TILs were stained using Calcein-AM according to the manufacturer's instructions. Seven thousand stained cells were suspended in Matrigel and human serum (05-720, Biological Industries) in a ratio of 0.5×10^6 cells to 20 μ L mix. The TIL mixture was supplemented with 3,000 IU/mL rhIL2. 20- μ L discs were solidified and transplanted on chorioallantoic membrane (CAM) from embryonic day 9 chicken eggs (E9 egg CAM) tangential to one another. Eggs (obtained from Wiessman henhouse) were then incubated at 37°C, 5% CO₂ for 24 hours and then imaged by stereomicroscope (Nikon, SMZ25), no filters were used.

Winn assay

Melanoma cells alone and a mixture (1:1) of melanoma and TILs were suspended in Matrigel and human serum in a ratio of 0.5×10^6 cells to 20 μ L mix. 20- μ L discs were solidified and transplanted on E9 egg CAM. After 24 hours or 48 hours tumors were excised, fixed in 4% paraformaldehyde and paraplast embedded. For immunohistochemistry staining, 6 μ m sections were stained with antibody specific for ADAR1 according to the manufacturer's protocol and then imaged at 40X magnification. For immunofluorescence 6 μ m sections were stained with DAPI and antibodies against ADAR1 followed by a secondary antibody all according to the manufacturer's protocol. Pictures were taken at 40 \times magnification.

ELISA

40,000 melanoma cells were seeded with TILs in 1:1 E:T ratio in a 96-well plate and incubated at 37°C, 5% CO₂ for 24h. Following incubation, supernatants were collected and processed using Human IFN- γ ELISA MAX (BLG-430104, Biolegend) according to manufacturer's instructions. Fluorescence was measured using Plate Reader GLOWMAX (Promega, WI USA).

Flow cytometry

Cells were washed and incubated with anti-B2M antibodies (Abcam Cat No. ab75853, RRID:AB_1523204) diluted in fluorescence-activated cell sorting medium (PBS, 0.02% sodium azide, and 0.5% BSA) for 30 minutes on ice. Following incubation, cells were washed and incubated with a secondary antibody (goat anti-rabbit IgG FITC, Thermo Fisher Scientific Cat No. 31635, RRID:AB_429708) for 30 minutes on ice. Following incubation cells were washed and collected for FACS analysis. All experiments were performed using a MACS-Quant instrument (Miltenybiotec) and analyzed using the MACS-Quantify software (version 2.13).

Western blotting

Melanoma cells were washed with PBS and lysed in RIPA (R0278, Sigma-Aldrich) lysis buffer and protease inhibitor cocktail (CST-5872S, Roche) on ice for 20 minutes. Insoluble material was removed by centrifugation at 14,000rpm for 10 minutes at 4°C. Protein concentration was measured using Pierce BCA protein kit (23225, Thermo Scientific). Proteins were separated by 6% SDS-PAGE, transferred onto Nitrocellulose membranes, embedded using 0.4%

paraformaldehyde and incubated with specific antibodies (ADAR1 (Sigma-Aldrich Cat No. HPA003890, RRID:AB_1078103), β -actin (Millipore Cat No. MAB1501, RRID:AB_2223041), total-STAT1 (Abcam Cat No. ab47425, RRID:AB_882708), STAT1 phosphorylated on Y701 (Abcam Cat No. ab29045, RRID:AB_778096)) over night at 4°C. Following incubation, the membranes were washed and secondary antibodies (goat anti-rabbit (Jackson ImmunoResearch Labs Cat No. 111-035-144, RRID:AB_2307391), goat anti-mouse (Jackson ImmunoResearch Labs Cat No. 115-035-146, RRID:AB_2307392)) were added for an incubation at room temperature for 1h. The antigen-antibody complexes were visualized by standard ECL reaction (20-500-1000, Biological Industries) and bands were developed on film (8194540, BioMax) using Carestream Medical X-ray processor.

Chemokine array

80,000 melanoma cells with ADAR1 knocked down or over-expressed and control were seeded in a 24-well plate and incubated at 37°C, 5% CO₂ for 48 h. Supernatants were collected and processed using The Proteome Profiler Human Chemokine Array (ARY017, R&D) according to manufacturer's instructions. Pixel density was measured using ImageJ (RRID:SCR_003070) and the data was expressed as a ratio of positive control of each membrane. The differential expression of chemokines was compared using nested ANOVA with the lme4 package (24) in R version 3.6. The p-values were adjusted for multiple comparisons using Benjamini-Hochberg. Chemokines were split by their cognate receptors and presented as clusters using the ComplexHeatmap package (RRID:SCR_017270) (25).

ADAR-p150 association with immune infiltration in melanoma transcriptomes

RNA from preimmunotherapy FFPE tumor biopsies of advanced melanoma patients treated with PD-1 blockade ($n = 36$) or TIL ACT ($n = 37$) was extracted with RNeasy FFPE Kit (73504, Qiagen). RNA sequencing (RNA-seq) libraries were prepared with Illumina's Ribo Zero Gold and TruSeq stranded library prep kits (RNA-seq_Macrogen, Macrogen Europe) and sequenced on the Illumina HiSeq2500 platform using paired-end sequencing with read length of 2 × 125–150bps. Reads were aligned to the human genome reference build hg19 using TopHat2 (RRID:SCR_013035) and were quantified with FeatureCounts (RRID:SCR_012919). ADAR-p150 expression was assessed by the number of reads, which aligned to the coding region that is unique to the ADAR1-p150 variant using bedtools coverage (RRID:SCR_006646). ADAR-p150 counts were added as a new feature to the raw count matrix. Raw counts were logCPM transformed. Immune infiltration was assessed by the ImmuneScore calculated in the ESTIMATE package in R. Pathway enrichment analysis of genes that strongly correlated with ADAR-p150 expression ($r_p > 0.4$) was performed by a hypergeometric test on Hallmark genesets which were downloaded from MsigDB. Raw data are available in supplementary Supplementary Table S2.

Association between chemokine expression, immune infiltration and survival

A correlation between *CCL3*, *CCL4*, *CCL5* expression and immune infiltration was calculated using the chemokines logCPM expression and the ImmuneScore, in our own immunotherapy-treated melanoma cohort (patients treated with PD-1 blockade ($n = 36$) or TIL ACT ($n = 37$)). Raw data are available in supplementary Supplementary Table S2.

In addition, association between chemokine expression and overall survival was assessed using the RNA-seq data from the TCGA skin cutaneous melanoma cohort ($n = 331$) by comparing the overall survival between samples with high (upper third) and low (lower third) *CCL3*, *CCL4* and *CCL5* log CPM expression using the log-rank test. The analysis was performed using R software environment. Further data regarding the skin cutaneous melanoma cohort including inclusion and exclusion criteria as previously published (26).

IHC, patient-derived biopsies

Tissues acquired by tumor biopsy were fixed in formalin for up to 24 hours and embedded into paraffin blocks. Blocks were sectioned at 4 μ m and stained against CD8 (Biocare Medical catalog no. CRM 311, RRID:AB_2750579), CD3 (Spring Bioscience catalog no. E1250, RRID:AB_1660773), CD68 (Agilent catalog no. M0876, RRID:AB_2074844), ADAR1, and HMB-45 according to the manufacturer's protocol. Images were acquired using Olympus microscope (BX60, serial NO. 7D04032) at objective magnification of X20 and microscope's Camera (Olympus DP73, serial NO. OH05504).

RNA-seq analysis of patient-derived biopsies

Previously published RNA-seq data (19) was reanalyzed using differential expression analysis of transcript-level or gene-level counts was performed on samples from 9 patients from the fecal microbiota transplantation cohort. ADAR1-p110 and ADAR1-p150 were differentiated as detailed below (*Quantifying ADAR1 transcripts*). To identify significant differential expression between post- and pretreatment groups, we used the paired Wald test and the raw count matrix as recommended from the DESeq2 standard analysis pipeline (RRID:SCR_015687).

Quantifying ADAR1 transcripts

To quantify ADAR1-p110 transcript abundances we used the cumulative counts of Ensembl IDs ENST00000648231, ENST00000368471, and ENST00000649022. To quantify ADAR-p150 transcript abundance we used the Ensembl ID ENST00000368474.

MicroRNA expression profile

RNA was extracted from mel624 with ADAR1 overexpression or mock using nCounter miRNA Assay Kit (CSO-MIR3-12, Nanostring) according to the manufacturer's instructions and analyzed using nCounter miRNA Expression Panel (NanoString). Full results are available in ArrayExpress (RRID:SCR_002964): accession number E-MTAB-11574.

RNA isolation and reverse transcription

Total RNA was isolated from melanoma cells (mel526, mel014, mel624) with ADAR knockdown using TriReagent (T9424, Sigma-Aldrich, Israel), and cDNA was generated by High-Capacity Reverse Transcriptase Kit (AB-4387406, Applied Biosystems, CA) using Universal Transcript cDNA Master Mix (ROCHE-05893151001, Roche, Switzerland) according to the manufacturer's instructions.

qRT-PCR

Primers (Sigma-Aldrich, Israel) were designed according to Primer-Express software guidelines (Applied Biosystems, CA). The qRT-PCR reactions were run in triplicates on LightCycler 480 system (Roche, Switzerland). Gene transcripts were detected using LightCycler 480 SYBR Green I Master (04887352001-1, Roche, Switzerland) according to the manufacturer's instructions. Reactions were normalized to

GAPDH. Relative expression was calculated using $2^{-\Delta\Delta Ct}$ equation. The detailed list of primers used for qRT-PCR follows:

ADAR1 p150: fw – CGGGCAATGCCTCGC rev – AATGGATGGGTGTAGTATCCG
IFNB: fw – CAGTTCAGAAAGGAGGACG rev – CTCAT-TCCAGCCAGTGCTA
CXCL9: fw – AAGGAACCCAGTAGTGA rev – CACATC-TGCTGAATCTGG
GAPDH: fw – TGCACCACCAACTGCTTAGC rev – GGCATG-GACTGTGGTCATGAG

Lactate dehydrogenase cytotoxicity assays

Cytotoxicity assays were performed by measuring lactate dehydrogenase (LDH) release, according to the manufacturer's instructions (CytoTox 96, Promega, catalog no. G1780). Briefly, target cells (melanoma cells) were co-incubated overnight with effector cells (TILs) at different E:T ratios in a 96-well plate. Forty-five minutes prior to harvesting supernatants, 10 μ L of lysis solution was added to a group of wells to obtain maximum LDH release. Plates were centrifuged and 50 μ L of supernatants were transferred to a fresh 96-well plate. 50 μ L of LDH substrate mix were added to each well and plates were incubated covered at room temperature. After 30 minutes, 50 μ L of stop buffer were added to each well. The LDH release was estimated by using a microplate reader (GloMax, Promega, Madison, WI) at 490 nm.

Statistics

Data was analyzed using the unpaired 2-tailed Student *t* test, the paired 2-tailed Student *t* test on log2 fold change, log-rank test and nested ANOVA. Correlations were examined with Pearson correlation test. $P \leq 0.05$ was considered significant.

Data availability

The data generated in this study are publicly available in ArrayExpress (RRID:SCR_002964), accession number E-MTAB-11574 or within the article and its Supplementary Data or from the corresponding author upon reasonable request. Read-level RNA-seq data are not available due to HIPAA protection. Any inquiries for accessing these data should be directed to the corresponding author and we will grant access to the deidentified data sets for research purposes.

Results

T-cell/melanoma interactions enhance chemotaxis in an MHC-I-restricted manner

To determine whether interactions between T cells and melanoma cells affect T-cell migration, we calculated the relative migration of TILs toward either melanoma cells alone or melanoma cells preincubated with cognate (HLA matching) TILs for 24 hours in a 1:1 E:T ratio. The responsiveness of cognate TILs was demonstrated by IFN γ release (Fig. 1A). Pre-exposure of melanoma cells to cognate TILs increased their chemo-attractive capacity, resulting in higher TIL migration in two of the three melanoma lines tested (mel526 and mel014; Fig. 1A). To further assess this effect, we analyzed TIL migration in fertilized chicken eggs where melanoma cells preincubated with cognate TILs (TIL014) or non-cognates TILs (TIL096) were seeded on the CAM with naïve TILs seeded between them. After 24 hours, the naïve TILs migrated more markedly to the side containing the melanoma cells preincubated with cognate TILs. This effect was observed in both mel526 and mel014 (Fig. 1B). To confirm that this effect is dependent on HLA recognition, the expression of β 2M, which

associates with MHC class I, was manipulated selectively. *B2M* was silenced in mel526 cells using siRNA or knocked out in mel14 using CRISPR technology, leading to downregulation of both β 2M and MHC class I within the manipulated cells (Fig. 1C). This abolished IFN γ release by cognate TILs in coculture experiments and diminished the cytotoxic effect, as assessed by LDH release, indicating the functional significance of β 2M manipulation (Fig. 1D; Supplementary Table S3). The β 2M manipulated melanoma cells preexposed to cognate TILs were further tested in migration assays and compared with mock-manipulated cells serving as negative control. Knockdown or knockout of *B2M* abrogated the enhanced migration after pre-exposure to TILs (Fig. 1D), indicating that the effect is MHC class I-restricted. Finally, melanoma cells were preincubated with an MHC-I-specific blocking monoclonal antibody (W6/32), which effectively reduced IFN γ secretion by the cocultured TILs (Fig. 1E) and abolished enhanced TIL migration (Fig. 1E), confirming that the effect is MHC class I-restricted.

The increase in chemotaxis is dependent on the IFN γ response

We hypothesized that the enhanced migration of TILs was dependent on the IFN γ response. Melanoma cultures were incubated with IFN γ R1 neutralizing antibody. TIL migration towards melanoma cells incubated with both the IFN γ R1 neutralizing antibody and cognate TIL for 24 hours in an E:T ratio of 1:1 was measured. Cells incubated with IC served as negative controls. Blocking IFN γ R1 eliminated the rise in migration after preexposure to cognate TILs (Fig. 2A), indicating that the IFN γ response was crucial for the migratory effect. Inhibition of the IFN γ response in the presence of the blocking antibody was confirmed by monitoring phosphorylated STAT1 (pSTAT1) levels (Fig. 2B). Protein samples from melanoma cells, generated from the migration assays described in Fig. 1, were similarly analyzed for pSTAT1 levels and a correlation between the migratory effect (Fig. 1) and IFN γ pathway activation (Fig. 2C and D) was confirmed.

To determine if IFN γ was functionally relevant to the chemotactic effect we incubated the melanoma cells with recombinant IFN γ for 24 hours. The migration assay was performed by washing the melanoma cells, replating them in a 96-well plate for 24 hours and seeding TILs in the transwell insert. Enhanced migration towards mel526 and mel624 was observed (Fig. 2E), supporting the role of IFN γ in promoting the chemo-attractive capacity of melanoma cells. An increase in pSTAT1 levels was confirmed (Fig. 2F). To further confirm this effect, melanoma cells preincubated with either IFN γ or vehicle for 24 hours were seeded on the CAM of fertilized chicken eggs with naïve TILs seeded between them for another 24 hours. Enhanced migration toward the side containing melanoma cells preincubated with IFN γ was observed (Fig. 2G). To further ascertain the role of the IFN γ pathway-response on TIL migration, the melanoma cells were incubated for 24 hours with the JAK1 and JAK2 inhibitor ruxolitinib (27) or they were treated with *JAK1*-specific siRNA. Then the melanoma cultures were exposed to IFN γ for 24 hours. Consistent with the abovementioned results, blocking of IFN γ pathway activation with ruxolitinib or with *JAK1*-knockdown, eliminated the rise in migration towards melanoma cells preexposed to IFN γ (Fig. 2H and J). Blockade of IFN γ pathway activation was evident by reduction in pSTAT1 levels in both experiments (Fig. 2I and K, respectively) while *JAK1* and *JAK2* expression remained constant in cells treated with ruxolitinib (Supplementary Fig. S1A) and reduced in cells treated with *JAK1*-specific siRNA (Fig. 2K). This collective evidence provides support for the role of IFN γ and activation of the IFN γ

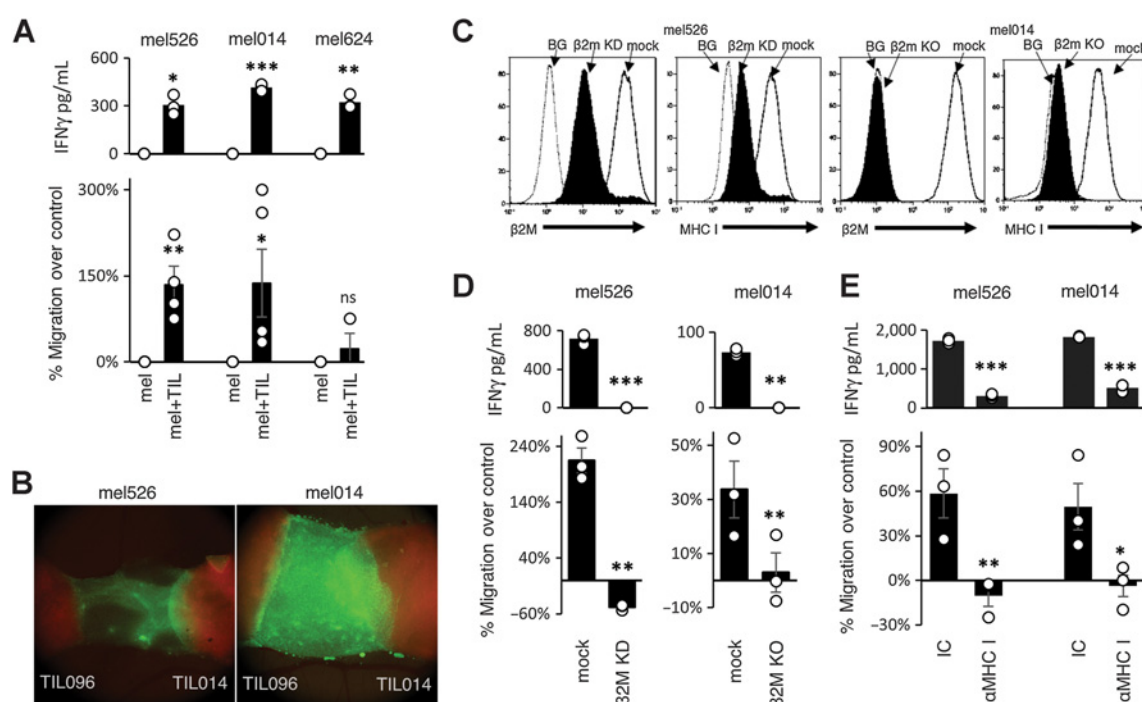


Figure 1.

T cell/melanoma interactions enhance chemotaxis in an MHC I-restricted manner. TIL migration toward melanoma cells previously cocultured with TILs. **A**, naïve melanoma cells (mel526 $n = 4$, mel014 $n = 4$, mel624 $n = 3$), **(D)** melanoma cells with $\beta 2m$ knockdown ($\beta 2m$ KD) or $\beta 2m$ knockout ($\beta 2m$ KO) ($n = 3$), or **(E)** melanoma cells incubated with neutralizing MHC I-specific antibody (αMHC I; $n = 3$) were cocultured with HLA-matching TILs. Quantification of IFN γ secretion (**A**, **D**, **E**; top). Melanoma cells were washed and seeded in the lower well of the Transwell system and TILs were seeded in the top chamber allowing them to migrate for 4 hours (**A**, **D**, **E**; bottom). The mean value of all independent experiments is shown as columns; error bars represent standard error of mean. **B**, TIL migration *in ovo* toward melanoma cells previously incubated with either cognate TILs (TIL014) or non-cognate TILs (TIL096) in a 1:1 E:T ratio. 7,000 melanoma cells previously cocultured with TILs for 24 hours were stained using Vybrant DiD and seeded on the CAM. 7,000 naïve TILs were stained using calcein AM and seeded between the two melanoma manipulations. TILs were allowed to migrate for 24 hours, a representative egg of at least 8 is shown. **C**, $\beta 2m$ and MHC I expression levels in $\beta 2m$ KD/KO cells, a representative experiment performed in triplicate is shown. *, $P < 0.05$; **, $P < 0.01$; ***, $P < 0.001$ by 2-tailed unpaired *t* test (**A**, top **D-E**), or 2-tailed paired *t* test on log₂ fold change (bottom **D-E**). BG, Background.

pathway in the increased chemoattraction of TILs by melanoma cells after pre-exposure to cognate TILs.

Increased chemotaxis is associated with induction of the ADAR1-p150 isoform in melanoma cells

To further investigate the underlying mechanism by which IFN γ response effects TIL migration we looked through IFN γ inducible genes for possible candidates. One gene known to play a major role in melanoma is *ADAR1*, which has an IFN-inducible isoform, p150. To check the association of ADAR1-p150 with immune infiltration, we quantified the reads that overlapped with the coding region unique to the ADAR1-p150 variant in RNA-seq data from tumor biopsies obtained from 73 patients with melanoma preimmunotherapy. We found that ADAR1-p150 had a significantly stronger correlation with ImmuneScore ($r_p = 0.44$, $P = 0.0001$) than ADAR ($r_p = 0.32$, $P = 0.007$; **Fig. 3A**). ImmuneScore was calculated by the ESTIMATE-R package that estimates the presence of infiltrating immune cells in tumor tissues using gene expression data. It is important to note that ADAR counts contain all variants including ADAR-p150 and therefore the actual correlation of non-p150-ADAR with immune infiltration is probably much lower (**Fig. 3A**). Moreover, pathway enrichment analysis for genes that were significantly correlated ($r_p > 0.4$) with ADAR-p150 highlighted the “Hallmark Interferon-gamma response” (Enrichment Factor =

13.5, adjusted P value < 0.0001) pathway, implying that ADAR1-p150 could be relevant to the migratory effect.

To investigate ADAR1-p150 expression dynamics, melanoma cultures were incubated with TILs and stained for ADAR1 expression. mel014 cells were cultured with TIL014 for 24 hours, then mounted onto a 3D matrix, fixed and stained with an ADAR1-specific antibody that targets both ADAR1 isoforms. Induction of cytoplasmic ADAR1, indicative of ADAR1-p150, was observed after 24 hours of incubation (**Fig. 3B**). mel526 and mel014 were implanted in a fertilized chick egg with either HLA-matched TILs (TIL014) or nonmatching TILs (TIL96) for 48 hours and then stained for ADAR1. ADAR1 expression increased in the cytoplasm of cells incubated with the HLA-matched TILs with no such induction observed with the nonmatching TILs (**Fig. 3B**). IFN γ pathway activation was confirmed by pSTAT1 (Supplementary Fig. S1B). To ascertain the relevance of ADAR1-p150 expression to TIL migration we investigated expression levels of ADAR1-p150 in protein samples from the migration assays depicted in **Figs. 1** and **2**. p150 was induced by recombinant IFN γ , and the induction was abolished in the presence of ruxolitinib (**Fig. 3C**). Induction of p150 was evident after exposure to cognate TILs, which was abrogated upon $\beta 2m$ downregulation or MHC class I blockade (**Fig. 3C**). The role of IFN γ was confirmed as p150 induction was neutralized by anti-IFN γ R1 (**Fig. 3C**). The induction in p150

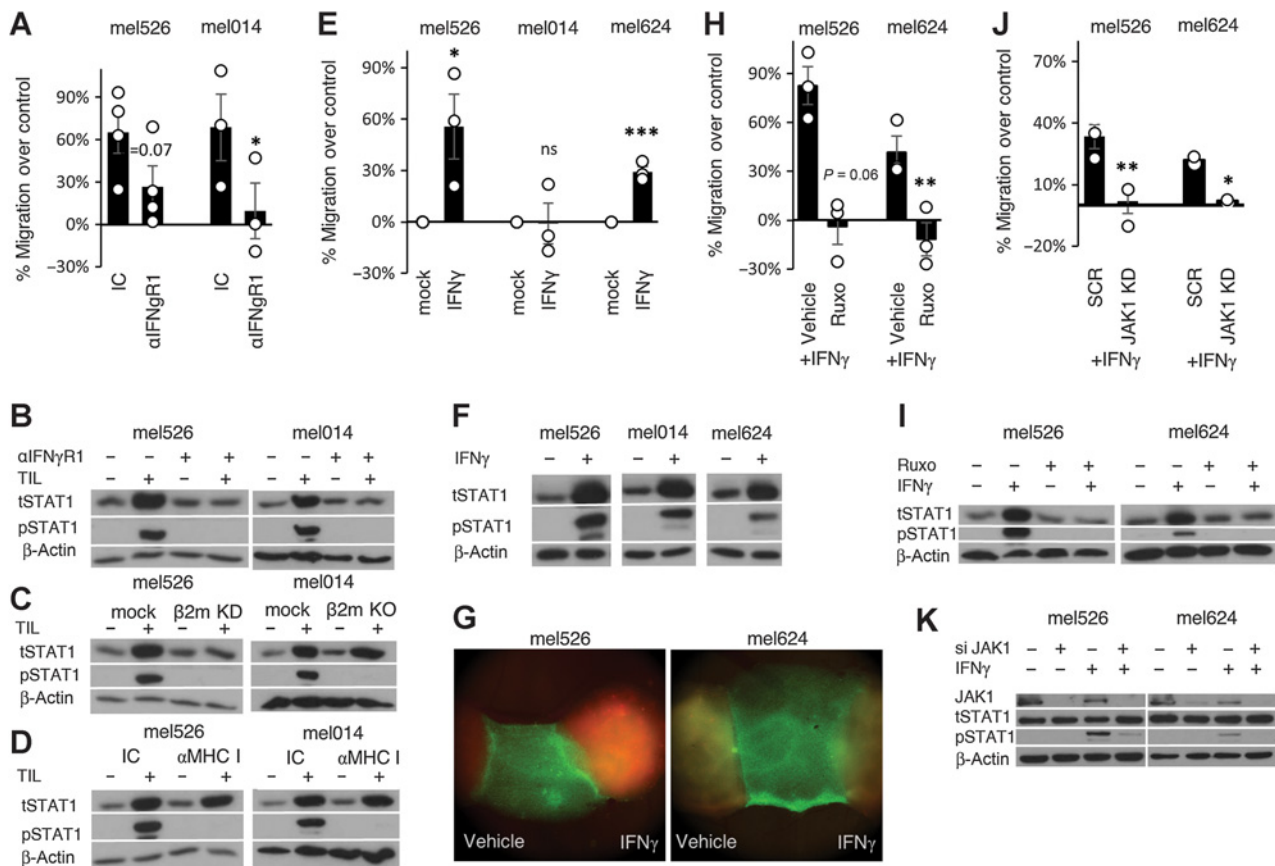


Figure 2.

The increase in chemotaxis is dependent on IFN γ response. TILs migration toward melanoma cells exposed to IFN γ . **A**, melanoma cells incubated with neutralizing anti-IFN γ R1 (α IFN γ R1) and TILs ($n = 3$), **(E)** melanoma cells incubated with recombinant IFN γ ($n = 3$), **(H)** melanoma cells incubated with recombinant IFN γ and ruxolitinib (Ruxo; $n = 3$), or **(J)** melanoma cells treated with JAK1-specific siRNA and recombinant IFN γ . Melanoma cells were washed and seeded in the lower well of the transwell system and TILs were seeded in the top chamber allowing them to migrate. The mean value of all independent experiments is shown as columns, error bars represent standard error of mean. **(B, C, D, F, I, K)** Expression of total STAT1 (tSTAT1) and phosphorylated STAT1 (pSTAT1), representative experiment performed in duplicate is shown. **F**, TIL migration *in ovo* toward melanoma cells previously incubated with either IFN γ (10 ng/mL) or vehicle. 7,000 melanoma cells previously incubated with IFN γ for 24 hours were stained using Vybrant DiD and seeded on the CAM. 7,000 naive TILs were stained using calcein AM and seeded between the two melanoma manipulations. TILs were allowed to migrate for 24 hours, a representative egg of at least 8 is shown. *, $P < 0.05$; **, $P < 0.01$; ***, $P < 0.001$ by 2-tailed unpaired t test **(E)**, or 2-tailed paired t test on log2 fold change **(A, H, J)**. KD, knockdown; KO, knockout; α MHC I, anti-MHC I antibody.

was evident also at the RNA level, following incubation with IFN γ (Supplementary Fig. S1C).

Both ADAR1 isoforms raise the chemotaxis potential of melanoma through a similar mechanism

To determine if ADAR1-p150 contributes to the increased T-cell migration, the p150 isoform was knocked-down in mel526 and mel624 cells, leaving the p110 isoform unaffected. Melanoma cultures with p150 knocked-down or mock manipulation were incubated for 24 hours with recombinant IFN γ and a migration assay was conducted. Knockdown of ADAR1-p150 abrogated the enhanced migration after preincubation with IFN γ towards both melanoma cell lines (Fig. 4A). Knockdown of ADAR1-p150 and its lack of response to IFN γ stimulation was confirmed at the protein level (Fig. 4B). The reduction in the migratory effect was confirmed in fertilized chicken eggs. Melanoma cells with p150 knocked-down or mock manipulation were incubated for 24 hours with either recombinant IFN γ or vehicle and seeded on the CAM with naive TILs between them for another 24 hours. The enhanced migration

after preincubation with IFN γ was abrogated by knockdown of ADAR1-p150 (Fig. 4C). These results indicated that ADAR1-p150 contributed to the enhanced TIL chemo-attraction.

To establish the role of ADAR1 in TIL migration, both the p110 and p150 isoforms were knocked down in mel526, mel014, and mel624 by stable shRNA transfection with a shared target sequence. Transfection with scramble shRNA served as negative control. In a migration assay was conducted using these melanoma cells, a significant decrease in migration was observed towards all three cell lines with ADAR1 knockdown compared with control (Fig. 4D). Knockdown of ADAR1 was confirmed at the protein level (Fig. 4E). These results indicate that a reduction in ADAR1 levels is sufficient to create a decrease in the chemo-attractive capacity of melanoma cells.

To determine if ADAR1-p110 can affect TIL migration, it was selectively overexpressed (OX) in mel526, mel014, and mel624, leaving expression of ADAR1-p150 unaffected. Transfection with an empty vector (Mock) served as control. In a migration assay, an increase in TIL migration was observed in all three cell lines overexpressing ADAR1-p110 compared with Mock (Fig. 4F). The selective

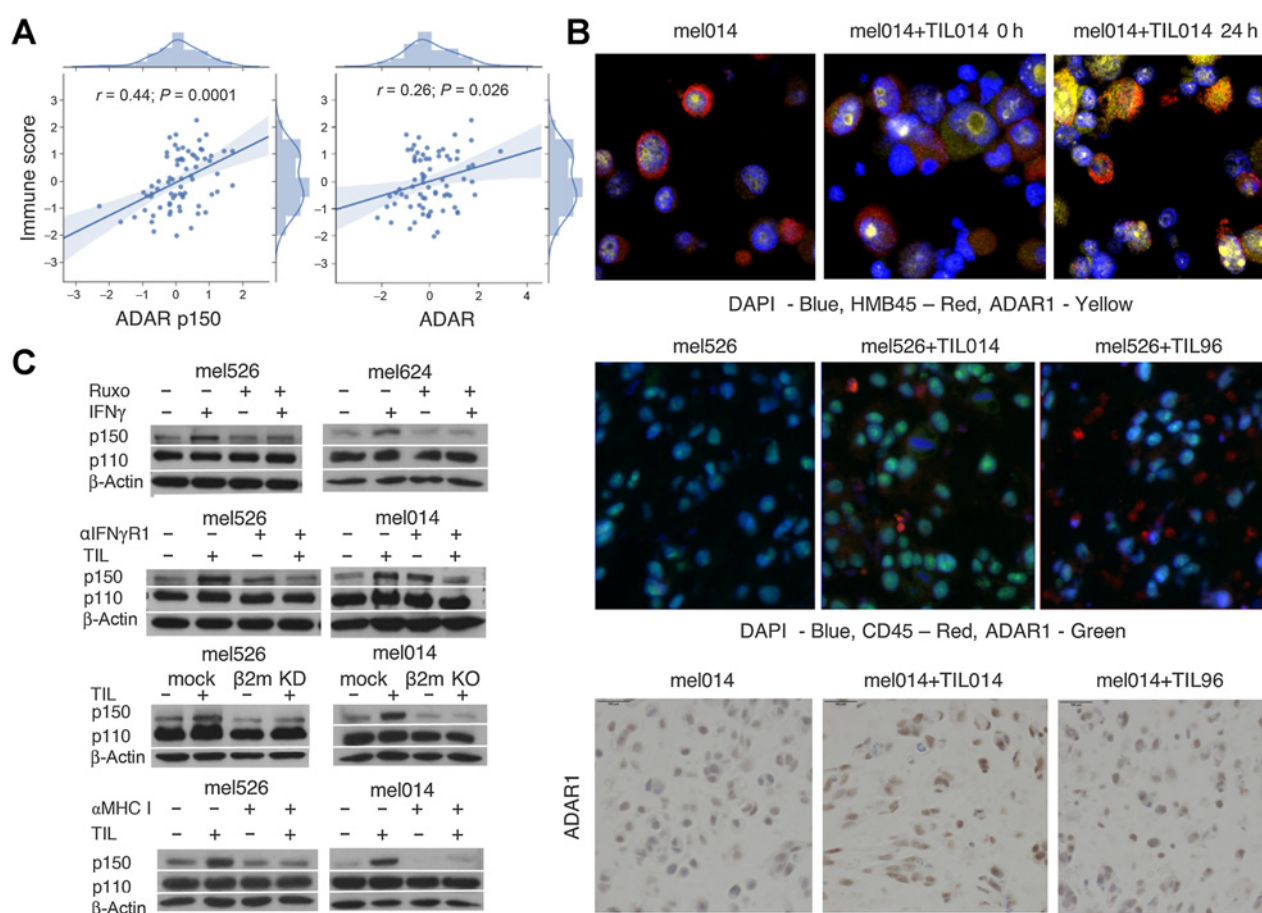


Figure 3.

The increase in chemotaxis is mediated through induction of the p150 isoform of ADAR1 in melanoma cells. **A**, Pearson correlation between the expression of ADAR1-p150 or total ADAR1 with ImmuneScore in preimmunotherapy tumor biopsies ($n = 73$). **B**, Immunofluorescence analysis of ADAR1 expression in melanoma cells cocultured with cognate TILs in a cell microarray (ICCM; top); coculture *in ovo* of melanoma cells with HLA-matching (TIL014) or nonmatching (TIL96) TILs analyzed by immunofluorescence (middle) or IHC (bottom). Stains are indicated in the figure. **C**, Western blot analysis of ADAR1 expression, both the long isoform (p150) and the short isoform (p110), a representative experiment performed in duplicate is shown of 3 performed. α MHC I, anti MHC I antibody; α IFN γ R1, anti-interferon gamma receptor 1 antibody; β 2M, beta-2-macroglobulin; KD, knockdown; KO, knockout; Ruxo, ruxolitinib.

overexpression was confirmed at the protein level (Fig. 4G). These results show that p110 alone, without incubation with either TILs or IFN γ , is capable of enhancing chemo-attraction of T cells.

To investigate the role of RNA-editing in the migratory effect, a mutation in the catalytic domain of ADAR1-p110 was introduced as previously described (15). The mutation was confirmed by sequencing. A migration assay was conducted using melanoma cultures with p110 OX containing a mutation in the catalytic domain, naïve p110 OX or Mock. A marked increase in TIL migration was observed for both the naïve p110 and the mutated p110, suggesting that ADAR1 affects TIL migration in an RNA editing-independent manner (Fig. 4H). The selective overexpression of ADAR1-p110 either naïve or containing the mutation in the catalytic domain was confirmed at the protein level (Fig. 4I).

To further assess the role of ADAR1 in the immune setting, ADAR1-manipulated cells were used as targets for TILs. As we have previously reported (16), ADAR1-OX renders cells significantly more sensitive to TIL killing in an RNA editing-independent manner, and ADAR1-knockdown cells are significantly more resistant to TIL killing (Supplementary Table S3).

Both knockdown of ADAR1 and exposure to IFN γ alter melanoma proliferation (15, 28). To verify that the difference in TIL migration we observed was not due to cellular arrest, three *ADAR1* null melanoma cell lines (mel526, mel014, mel624) were incubated with recombinant IFN γ or vehicle. The cells were seeded following the exact timeline of the migration protocol and counted at the time the migration would be initiated. No significant difference was observed for all cell lines (Supplementary Fig. S1D).

ADAR1 alters the chemokine expression profile produced by melanoma cells

To determine if ADAR affects chemotaxis through alterations in chemokine expression, melanoma cultures with either *ADAR1* knocked down or *ADAR1*-p110 overexpressed were plated for 48 hours. The conditioned media were collected and analyzed for chemokine and cytokine expression using a semi-quantified chemokine array. Protein levels were analyzed by ImageJ. Mock cells were used as negative control and the relative expression was calculated as the ratio between the expression in the manipulated cells and the mock cells. A strong decrease in the production of the chemokine ligands for

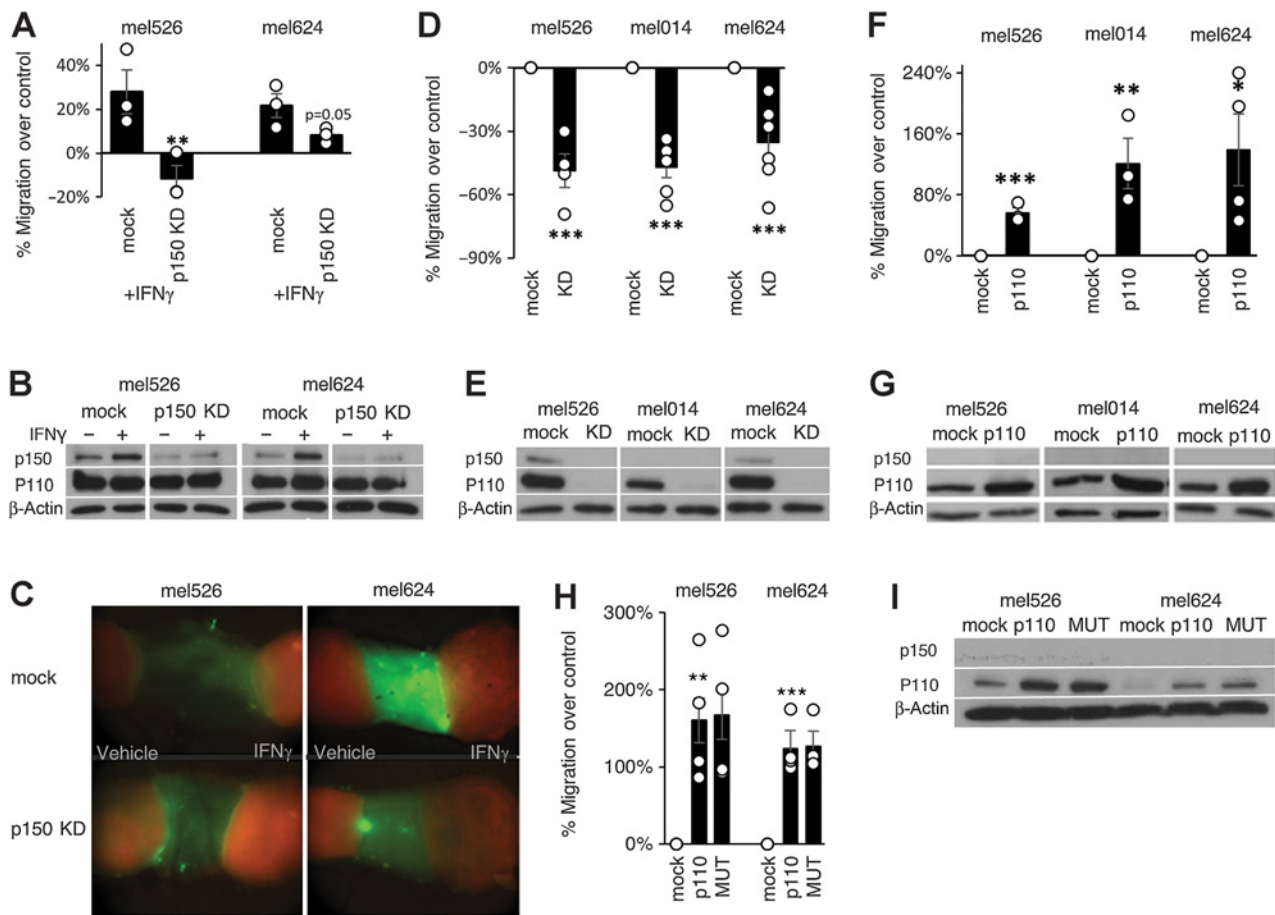


Figure 4. Both ADAR1 isoforms raise the chemotaxis potential of melanoma cells through a similar mechanism. TIL migration toward melanoma cells with (A) ADAR1-p150 KD incubated with IFN γ ($n = 3$), (D) ADAR1 knockdown (mel526 $n = 3$, mel014 $n = 6$, mel624 $n = 7$), (F) ADAR1-p110 overexpression (mel526 $n = 3$, mel014 $n = 3$, mel624 $n = 4$), or (H) ADAR1-p110 overexpression with a mutation in the catalytic domain ($n = 3$). Melanoma cells were seeded in the lower well of the transwell system and TILs were seeded in the top chamber allowing them to migrate for 4 hours. The mean value of all independent experiments is shown as columns, error bars represent standard error of mean. (B, E, G, I) ADAR1 expression for both the long isoform (p150) and the short isoform (p110), a representative experiment performed in duplicate of at least 3 performed is shown. C, TIL migration *in vivo* toward melanoma cells with knockdown of ADAR1-p150 or mock previously incubated with either IFN γ (10 ng/mL) or vehicle. 7,000 melanoma cells previously incubated with IFN γ for 24 hours were stained using Vybrant DiD and seeded on the CAM. 7,000 naive TILs were stained using calcein AM and seeded between the two melanoma manipulations. TILs were allowed to migrate for 24 hours, a representative egg of at least 8 is shown. *, $P < 0.05$; **, $P < 0.01$; ***, $P < 0.001$ by 2-tailed unpaired t test (D, F, H), or 2-tailed paired t test on log2 fold change (A). KD, knockdown.

CCR4, CCR5, and CXCR3 was observed in the ADAR1 knockdown cells, whereas the opposite effect, an increase, was observed in the ADAR1-p110 overexpressing cells (Fig. 5A). Multiple other chemokines and cytokines were altered as well (Supplementary Fig. S2). This suggests that ADAR1 controls the chemo-attractive capacity of melanoma cells by altering chemokine expression levels.

It was previously reported that there is an upregulation of several chemokines in ADAR-null cells following IFN stimulation (29). To further investigate the combined effect of IFN γ and ADAR1 downregulation on human melanoma cell lines, three cell lines (mel526, mel014, and mel624) with ADAR1 knocked down were incubated with IFN γ for 48 hours followed by RNA extraction and quantification of *IFNB* and *CXCL9* expression. There was a mild induction in the expression of *IFNB* and a strong induction of *CXCL9* following IFN γ stimulation, but no significant difference was observed between ADAR1 knockdown cells and their controls (Supplementary Fig. S3).

Next, migration assays were performed using melanoma cultures with ADAR1-p110 overexpression and TILs preincubated with chemokine receptor antagonists against CCR4, CCR5, and CXCR3 (aCCRs). Blocking the chemokine receptors on TILs eliminated the increase in migration caused by ADAR1-p110 overexpression (Fig. 5B). Next, melanoma cultures were incubated with IFN γ for 24 hours and then seeded for a migration assay with TILs preincubated with aCCRs. Consistent with the abovementioned results, blocking the chemokine receptors on TILs eliminated the increase in migration (Fig. 5C). Collectively, these results suggest that ADAR1 controls chemokine production by melanoma cells, thereby governing the TIL migratory effect.

Three of CXCR3 chemokine ligands are directly induced by IFN γ : CXCL9, CXCL10, and CXCL11 (8). Therefore, these chemokines may contribute to the IFN γ -driven enhanced migration (Figs. 1 and 2) in an ADAR1-independent manner. CCR5 has three main ligands—CCL3, CCL4, and CCL5 (30)—which are not induced directly by IFN γ .

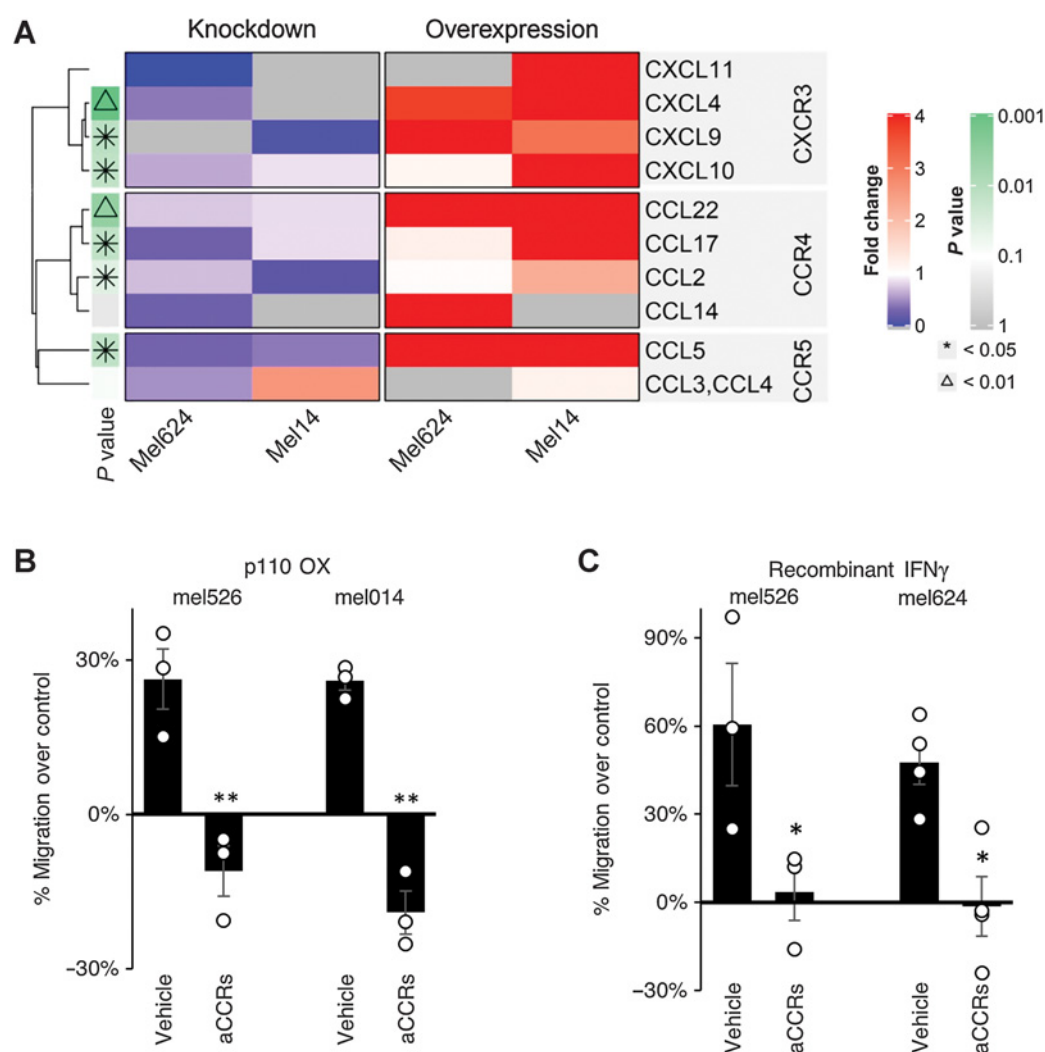


Figure 5.

ADAR1 alters the chemokine expression profile thus affecting the chemotaxis of T cells toward melanoma cells. **A**, The culture medium of two cell lines with either *ADAR1* knocked-down or *ADAR1*-p110 overexpressed was collected and analyzed for chemokine expression profile. **B** and **C**, TIL migration toward melanoma cells with either (**B**) *ADAR1*-p110 overexpression (mel526 $n = 3$, mel014 $n = 3$) or (**C**) naïve cells incubated with recombinant $\text{IFN}\gamma$ (mel526 $n = 3$, mel624 $n = 4$). Melanoma cells were seeded in the lower well of the transwell system and TILs were incubated with chemokine receptor antagonists against CCR4, CCR5, and CXCR3 (aCCRs) and then placed in the top chamber allowing them to migrate for 4 hours. The mean value of all independent experiments is shown as columns, error bars represent standard error of mean. (**A**) *, $P < 0.05$; $\Delta P < 0.01$ by nested ANOVA. P values were adjusted for multiple comparisons. (**B**, **C**) *, $P < 0.05$; **, $P < 0.01$, by 2-tailed paired t test on \log_2 fold change.

We found that survival analysis on data from the TCGA skin cutaneous melanoma cohort revealed strong correlations between chemokine expression levels and survival (**Fig. 6A**) and between chemokine expression and ImmuneScore (**Fig. 6B**). The expression patterns in the chemokine array point to the correspondence between CCL5 pattern and the migratory effect (**Fig. 5A**). To verify the functional relevance of CCL5, TIL migration was tested towards *ADAR1* knockdown melanoma cell lines with or without recombinant CCL5 in the lower well. We observed that CCL5 successfully negated the reduced TIL migration towards melanoma cells conferred by *ADAR1* knockdown (**Fig. 6C**). Next, the effect of CCL4 was tested on TIL migration towards *ADAR1* knockdown melanoma cells. CCL4 was overexpressed in *ADAR1* knockdown cells, and transfection of empty vector served as control. Even though CCL4 was not significantly correlated with *ADAR1* expression (**Fig. 5A**), its overexpression was enough to

negate reduced migration conferred by *ADAR1* knockdown (**Fig. 6D**). Taken together, these results show that the change in chemokine expression induced by *ADAR1* has a pivotal role in TIL migration.

We have previously shown that *ADAR1* affects many cellular processes by modulating microRNA expression (15, 16). Comparative microRNA expression profiles were generated for mel624 cells with *ADAR1* knocked down versus control and for mel624 cells overexpressing *ADAR1*-p110 versus control. The two differential microRNA profiles were crossed with the microRNAs that target either CCL4 or CCL5, using the current target prediction database, miRDB (31). We found that *ADAR1* knockdown reduced some CCL4- and CCL5-targeting microRNAs, whereas *ADAR1*-p110 overexpression increased other CCL4- and CCL5-targeting microRNAs (**Fig. 6E**). This pattern is not unique to chemokines that bind to receptors present on TILs (7) as a similar pattern was observed for CCL1 and CXCL7

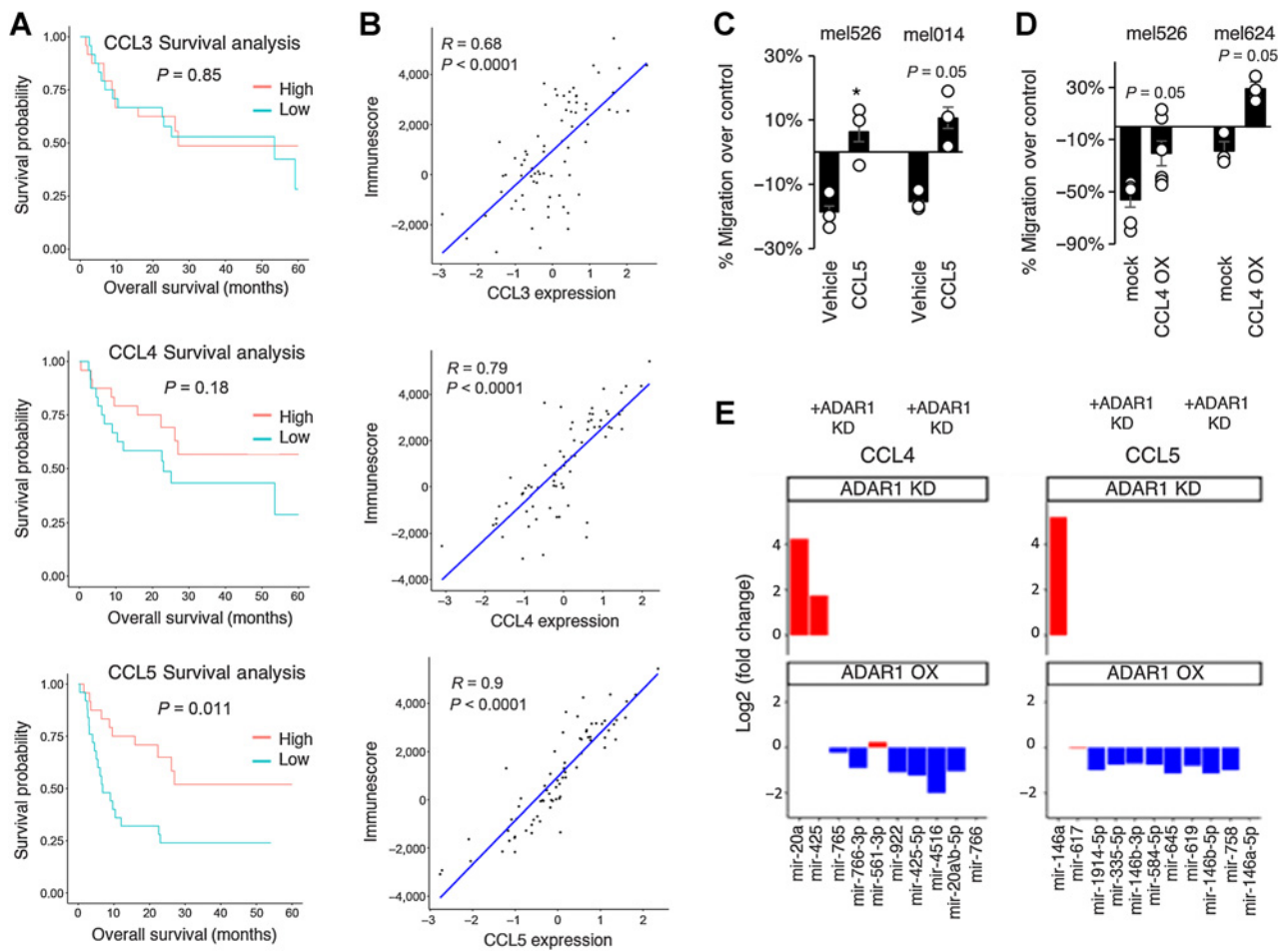


Figure 6.

The expression of CCL3, CCL4, and CCL5 is altered via ADAR1, affecting both survival and T-cell migration. **A** and **B**, Association between chemokine expression levels and survival (**A**) or ImmuneScore (**B**) in patients with melanoma. Overall survival of melanoma patients by CCL3, CCL4, and CCL5 expression ($n = 73$). **C**, TIL migration toward melanoma cells with *ADAR1* knockdown incubated with recombinant CCL5 100 ng/mL ($n = 3$) or (**D**) melanoma cells with *ADAR1* knockdown and overexpression of CCL4 (mel526 $n = 6$, mel624 $n = 3$). Melanoma cells were seeded in the lower well of the transwell system and TILs in the top chamber allowing them to migrate for 4 hours. The mean value of all independent experiments is shown as columns, error bars represent standard error of mean. **E**, Change in microRNA expression levels in *ADAR1* knockdown compared with its mock control or in *ADAR1*-p110 overexpression compared with its mock control regarding microRNAs that are predicted to target either *CCL4* or *CCL5*. Statistical analysis was performed using logrank test (**A**) or by 2-tailed paired *t* test on log2 fold change, *, $P < 0.05$; **, $P < 0.01$ (**B** and **C**).

(Supplementary Fig. S4) which bind to CCR8 and CXCR2, respectively, and are not expressed by TILs (7, 32). The expression of microRNAs is aligned with the expression levels of the four chemokines in *ADAR1* knockdown or *ADAR1*-p110 overexpressing melanoma cells (Fig. 5).

Fecal microbiota transplant alters ADAR1 expression in metastatic melanoma patient

To further investigate the relevance of our findings in the clinical setting, tumor biopsies from two metastatic melanoma patients were stained for ADAR1 expression. Biopsies were obtained from the patients before and after treatment with FMT alongside anti-PD-1 immunotherapy as described (19). We found that ADAR1 induction occurs *in situ* (Fig. 7A). Three different fields were captured from each biopsy (Supplementary Fig. S5). In an analysis conducted on the entire FMT cohort ($N = 10$), in patients that responded to reinduction of immunotherapy following the FMT, a rise in ADAR1-p150 but not ADAR1-p110 RNA expression was observed (Fig. 7B). Staining of CD3, CD8, and

CD68 in sequential slides of the same abovementioned biopsies revealed an influx of immune cells following FMT (Fig. 7C). The differences between baseline and posttreatment immune cell counts were correlated with the differences in total ADAR1, ADAR1-p110, and ADAR1-p150 RNA expression. The only statistically significant correlation was between the change in ADAR1-p150 expression and CD8⁺ counts (Fig. 7D). On the basis of all the experimental evidence described above, it is possible that ADAR1 induction plays a role in this increased infiltration and reinvigorated the antimelanoma immune response.

Discussion

Immune infiltration is a key factor in the response to immunotherapy, as tumors lacking T-cell infiltration ("cold" tumors) are typically less responsive to immunotherapy (33). On the other hand, the presence of T cells at the tumor margin is significantly associated with response to anti-PD-1 therapy (1). The clinical tumor regression

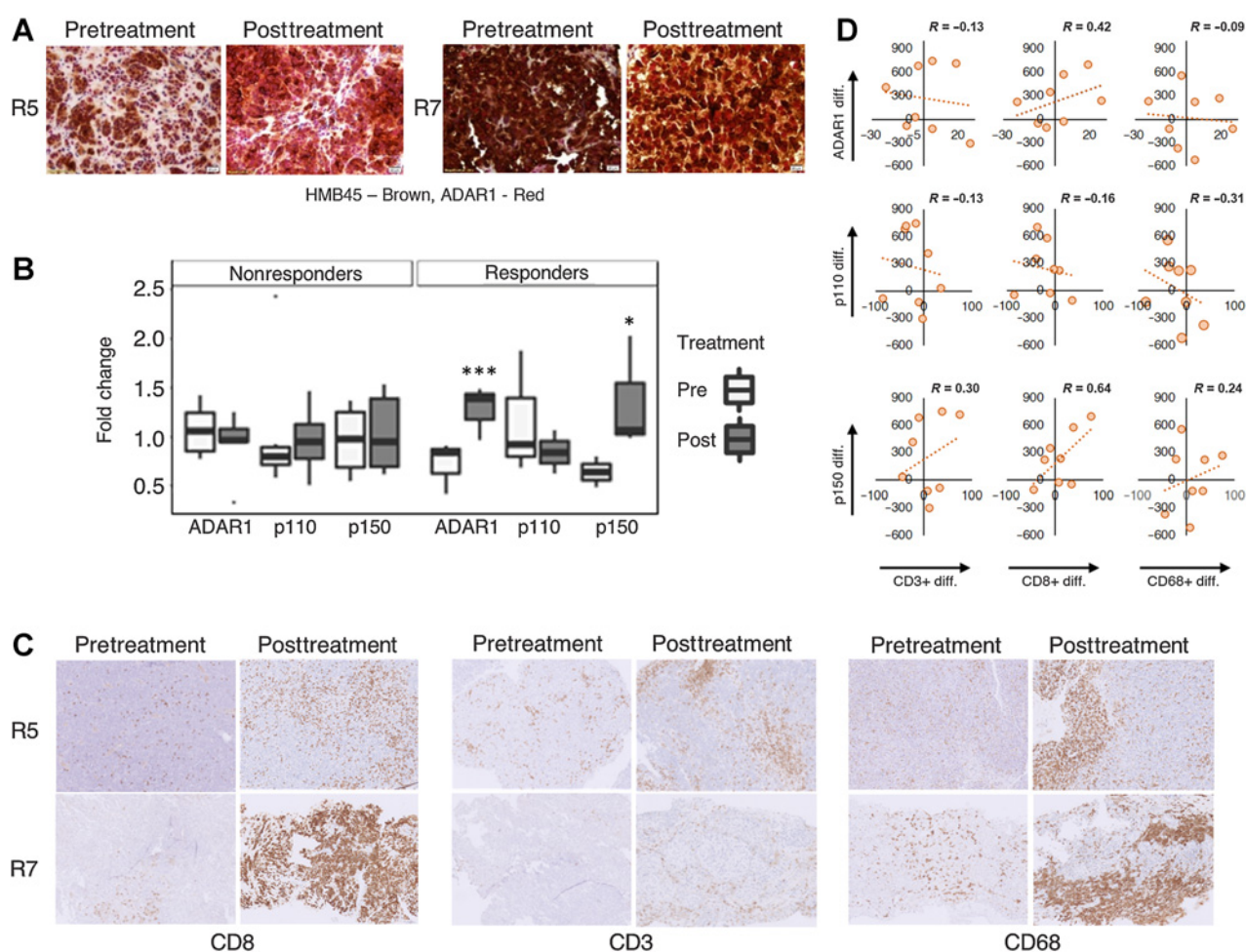


Figure 7.

Fecal microbiota transplantation alters ADAR1 expression in metastatic melanoma recipient patient. **A**, Immunohistochemistry staining of ADAR1 (red) and HMB-45 (brown) in two biopsies from two patients with metastatic melanoma before and after fecal microbiota transplantation (FMT). **B**, RNA-seq analysis of patient-derived biopsies. Differential expression analysis of transcription-level or gene-level was performed on samples from nine patients from the FMT cohort (three responders and six nonresponders). Statistical analysis was done using the paired Wald-test and the raw count matrix, *, $P < 0.05$. **C**, IHC staining of either CD8, CD3, or CD68 in two biopsies from two patients with metastatic melanoma before and after FMT. **D**, Correlation analysis between the difference in expression of either ADAR1, ADAR1-p110, or ADAR1-p150 before and after FMT with the difference in immune infiltration (as seen in the difference in expression of either CD8, CD3, or CD68).

mediated by PD-1-axis blockade is typically followed by enhanced immune infiltration, which is considered to mediate the main clinical effect (1, 34, 35). The drivers of the immune infiltration are still mostly unknown. Here, we offer a mechanism for this in which direct antigen-specific melanoma/T-cell interactions alter the melanoma cells, causing them to attract more T cells.

First, we provide substantial evidence that MHC-I-restricted interactions between T cells and the melanoma cells enhance the chemo-attractive capacity of the melanoma cells. We showed this through selective MHC class I downregulation at the genetic and mRNA levels, as well as functionally by using blocking monoclonal antibodies. Moreover, we showed that it is $\text{IFN}\gamma$ released from the T cells following antigen-restricted recognition (36) that drives the enhanced T-cell migration through activation of the $\text{IFN}\gamma$ pathway in the melanoma cells. We showed that exogenous $\text{IFN}\gamma$ recapitulated the enhanced migration effect and that interference using blocking anti- $\text{IFN}\gamma$ antibodies or the JAK1/JAK2 inhibitor ruxolitinib abolished the effect. These results suggest a positive feedback loop, in which target-cell

recognition directly leads to the recruitment of additional T cells. The correlation between IFN -signature and immune infiltration, survival and response to immunotherapy has been demonstrated in different tumors (37) with the typical interpretation that it reflects an ongoing favorable immune response. Our results point to an underlying mechanism: T cells at the tumor margin could drive the melanoma cells to have a greater chemo-attractive capacity thereby creating an influx of new T cells. This phenomenon could also account for the increased T-cell influx following anti-PD-1 therapy.

$\text{IFN}\gamma$ pathway activation leads to the transcriptional induction of multiple ISG through the JAK1/2-STAT1 pathway (5). Here, we showed that ADAR1-p150 is induced in melanoma cells upon antigen-restricted recognition by T cells via $\text{IFN}\gamma$ and that its expression is significantly correlated with T-cell infiltration in 73 melanoma specimens. ADAR1-p150 was responsible for the enhanced $\text{IFN}\gamma$ -driven migration, as its selective knockdown abrogated the effect. By silencing or overexpression of the constitutive ADAR1 isoform, p110, we showed that p110 controls the chemo-attractive capacity of melanoma cells in a similar manner.

Thus, while chemo-attraction is constitutively regulated by ADAR1-p110, it can adaptively alter through the expression levels of ADAR1-p150.

Our results are opposite to those reported by Ishizuka and colleagues, who demonstrated in murine models higher tumor T-cell infiltration in ADAR1-null mice along with melanoma cell arrest (29). The decrease in chemokine expression we described in ADAR1 knocked down cells could be a result of a PKR-mediated translational arrest that precedes cell death. Although this remains a possibility that should be explored in the future, we and others have previously shown that ADAR1 loss in human melanoma actually causes enhanced proliferation (15), invasion (38), and metastasis (39), with no similar effects in murine melanoma (29). Thus, ADAR1 may have differential effects on T-cell migration in humans and mice. One possible explanation for this discrepancy is the difference in frequency of A-to-I editing, as there is at least an order of magnitude more of these editing events in humans than in mice (40). Other explanations could be differential effects on microRNA biogenesis through RNA editing-independent mechanisms, but this remains to be further investigated.

Biopsies from metastatic melanoma tumor sites revealed a correlation between six chemokines and lymphocyte infiltration (41). These chemokines correspond with the most abundant chemokine receptors among melanoma-derived TIL cells – CXCR3, CCR5, and CCR4 (7). We found that CCL3, CCL4 and CCL5 are strongly correlated with T-cell infiltration and patient survival. In addition, we showed that ADAR1 enhances the expression of all these chemokines. Thus, IFN γ -driven induction of ADAR1-p150 presumably enhances their expression and thereby T-cell chemo-attraction. Indeed, migration of T cells towards melanoma cells treated with IFN γ or ADAR1-p110 overexpression was abolished in the presence of the appropriate chemokine receptor antagonists. Moreover, exogenous addition or forced expression of the chemokines CCL5 or CCL4, respectively, negated the inhibitory effect conferred by ADAR1 silencing.

The collective evidence presented here suggest that both ADAR1-p110 and ADAR1-p150 alter migration through a similar mechanism, potentially through microRNAs. It is unclear why *ADAR1* knockdown or overexpression altered different chemokine-targeting microRNAs. ADAR1 controls microRNA biogenesis through several mechanisms, including pri- or pre-miR binding or DGCR8 protein-binding (15). We propose that differential sensitivity of these mechanisms to ADAR1 levels accounts for this observation, which merits further investigation.

The evidence presented here suggest that ADAR1-p110 and ADAR1-p150 play different roles in the tumor-immune system interrelationship. The downregulation of ADAR1-p110 occurs in the transition from primary to metastatic melanoma due to inherent genetic and epigenetic mechanisms within the melanoma cells, and it contributes to immune exclusion. However, IFN γ secreted by antigen-specific T cells that interact with melanoma cells, forces the melanoma cells to induce ADAR1-p150. By inducing ADAR1-p150, chemokine production is restored, the chemo-attraction signal for T cells increases, and immune exclusion is reduced. It is plausible this mechanism mediates the facilitated immune infiltration following PD-1-axis blockade or in pseudo-progression following immunotherapy. It has been shown that response to anti-PD-1 is associated with T-cell infiltration subsequent to the treatment (42). As PD-1 blockade doesn't lead by itself to increased chemotaxis, our results provide a potential explanation for that important phenomenon. We speculate that PD-1 blockade alleviates, at least in part, the inhibition from tumor-residing antigen-specific T cells, leading to the release of IFN γ and triggering the ADAR-p150-dependent chemo-attraction of T cells. Thus, the effect is dependent on the residual ability of the tumor cells to respond to IFN γ , so ADAR1-p150 could be induced. This is in

agreement with clinical data showing that response to immunotherapy is strongly correlated with IFN responsiveness (37). The rise in ADAR1 expression that we observed in metastatic melanoma patients after FMT and anti-PD-1 therapy, along with the rise in CD8⁺ infiltration (19), may provide preliminary support for this hypothesis. Further investigation is mandated to establish the involvement of this entire cascade in clinical scenarios.

ADAR1 plays a dual role in cancer and has both oncogenic and tumor suppressive effects in different malignancies (43). For instance, in contrast to the role of ADAR1 in human melanoma (15, 16, 38, 39), ADAR1 is over expressed and promotes cancer progression in lung cancer, liver cancer, esophageal cancer, and chronic myelogenous leukemia (44–46). This may seem contradictory at times, however, it emphasizes the involvement of ADAR1 in many different cellular pathways (43). Because of this multilayered effect that is also tissue specific, it is difficult to speculate the relevance of the migratory effect governed by ADAR1 in other malignancies.

In conclusion, we suggest that the downregulation of the constitutive ADAR1-p110 during melanoma transition from primary to metastatic disease reduces lymphocyte chemo-attraction and contributes to the development of a “cold tumor” phenotype. On the other hand, antigen-restricted recognition of melanoma cells by T cells causes an IFN γ -driven induction of ADAR1-p150, which restores chemo-attraction and increases the antigen-restricted interactions. This positive feedback mechanism may play a central role in the development of hot tumors and successful response to immunotherapy.

Authors' Disclosures

N. Margolis reports grants from Israel Science Foundation IPMP; and grants from Samuelli Foundation during the conduct of the study. H. Moalem reports grants from Israel Science Foundation; and grants from Samuelli Foundation during the conduct of the study. T. Meirson reports personal fees from TyrNovo outside the submitted work. B. Vizel reports grants from Israel Science Foundation; and grants from Samuelli Foundation during the conduct of the study. M.J. Besser reports personal fees from KSQ Therapeutics, Gilboa Therapeutics, Sartorius; and personal fees from MSD outside the submitted work. G. Markel reports grants from Israel Science foundation; and grants from Samuelli Foundation during the conduct of the study; personal fees from 4C Biomed, Starget, NucleAI, BeyondAir, MSD, Roche; grants and personal fees from BMS, Novartis; and grants and personal fees from Sanofi outside the submitted work. No disclosures were reported by the other authors.

Authors' Contributions

N. Margolis: Conceptualization, formal analysis, investigation, methodology, writing—original draft. H. Moalem: Investigation. T. Meirson: Data curation, formal analysis. G. Galore-Haskel: Investigation, methodology. E. Markovits: Data curation, formal analysis, investigation. E.N. Baruch: Investigation. B. Vizel: Methodology. A. Yeffet: Investigation. J. Kanterman-Rifman: Investigation. A. Debby: Investigation. M.J. Besser: Resources. J. Schachter: Resources. G. Markel: Conceptualization, resources, formal analysis, supervision, funding acquisition, validation, methodology, writing—original draft, writing—review and editing.

Acknowledgments

G. Markel was supported by grant from Israel Science foundation (IPMP 3956) and grant for integrative immuno-oncology from the Samuelli Foundation.

The costs of publication of this article were defrayed in part by the payment of page charges. This article must therefore be hereby marked *advertisement* in accordance with 18 U.S.C. Section 1734 solely to indicate this fact.

Note

Supplementary data for this article are available at Cancer Immunology Research Online (<http://cancerimmunolres.aacrjournals.org/>).

Received August 17, 2021; revised January 10, 2022; accepted June 14, 2022; published first June 21, 2022.

References

1. Tumei PC, Harview CL, Yearley JH, Shintaku IP, Taylor EJM, Robert L, et al. PD-1 blockade induces responses by inhibiting adaptive immune resistance. *Nature* 2014;515:568–71.
2. Johnson KG, Bromley SK, Dustin ML, Thomas ML. A supramolecular basis for CD45 tyrosine phosphatase regulation in sustained T-cell activation. *Proc Natl Acad Sci U S A* 2000;97:10138–43.
3. Freiberg BA, Kupfer H, Maslanik W, Delli J, Kappler J, Zaller DM, et al. Staging and resetting T-cell activation in SMACs. *Nat Immunol* 2002;3:911–7.
4. Bhat P, Leggat G, Waterhouse N, Frazer IH. Interferon- γ derived from cytotoxic lymphocytes directly enhances their motility and cytotoxicity. *Cell Death Dis* 2017;8:e2836.
5. Castro F, Cardoso AP, Gonçalves RM, Serre K, Oliveira MJ. Interferon-gamma at the crossroads of tumor immune surveillance or evasion. *Front Immunol* 2018;9:847.
6. Schneider WM, Chevillotte MD, Rice CM. Interferon-stimulated genes: a complex web of host defenses. *Annu Rev Immunol* 2014;32:513–45.
7. Sapoznik S, Ortenberg R, Galore-Haskel G, Kozlovski S, Levy D, Avivi C, et al. CXCR1 as a novel target for directing reactive T cells toward melanoma: implications for adoptive cell transfer immunotherapy. *Cancer Immunol Immunother* 2012;61:1833–47.
8. Kanda N, Shimizu T, Tada Y, Watanabe S. IL18 enhances IFN γ -induced production of CXCL9, CXCL10, and CXCL11 in human keratinocytes. *Eur J Immunol* 2007;37:338–50.
9. Zinshteyn B, Nishikura K. Adenosine-to-inosine RNA editing. *Wiley Interdiscip Rev Syst Biol Med* 2009;1:202–9.
10. Maas S, Rich A, Nishikura K. A-to-I RNA editing: recent news and residual mysteries. *J Biol Chem* 2003;278:1391–4.
11. Levanon EY, Eisenberg E, Yelin R, Nemzer S, Halleger M, Shemesh R, et al. Systematic identification of abundant A-to-I editing sites in the human transcriptome. *Nat Biotechnol* 2004;22:1001–5.
12. Kim DDY, Kim TTY, Walsh T, Kobayashi Y, Matisse TC, Buyske S, et al. Widespread RNA editing of embedded Alu elements in the human transcriptome. *Genome Res* 2004;14:1719–25.
13. Blow MJ, Grocock RJ, van Dongen S, Enright AJ, Dicks E, Futrelt PA, et al. RNA editing of human microRNAs. *Genome Biol* 2006;7:R27.
14. Kawahara Y, Zinshteyn B, Sethupathy P, Iizasa H, Hatzigeorgiou AG, Nishikura K. Redirection of silencing targets by adenosine-to-inosine editing of miRNAs. *Science* 2007;315:1137–40.
15. Nemlich Y, Greenberg E, Ortenberg R, Besser MJ, Barshack I, Jacob-Hirsch J, et al. MicroRNA-mediated loss of ADAR1 in metastatic melanoma promotes tumor growth. *J Clin Invest* 2013;123:2703–18.
16. Galore-Haskel G, Nemlich Y, Greenberg E, Ashkenazi S, Hakim M, Itzhaki O, et al. A novel immune resistance mechanism of melanoma cells controlled by the ADAR1 enzyme. *Oncotarget* 2015;6:28999–9015.
17. Besser MJ, Shapira-Frommer R, Treves AJ, Zippel D, Itzhaki O, Hershkovitz L, et al. Clinical responses in a phase II study using adoptive transfer of short-term cultured tumor infiltration lymphocytes in metastatic melanoma patients. *Clin Cancer Res* 2010;16:2646–55.
18. Besser MJ, Shapira-Frommer R, Itzhaki O, Treves AJ, Zippel DB, Levy D, et al. Adoptive transfer of tumor-infiltrating lymphocytes in patients with metastatic melanoma: intent-to-treat analysis and efficacy after failure to prior immunotherapies. *Clin Cancer Res* 2013;19:4792–800.
19. Baruch EN, Youngster I, Ben-Betzalel G, Ortenberg R, Lahat A, Katz L, et al. Fecal microbiota transplant promotes response in immunotherapy-refractory melanoma patients. *Science* 2021;371:602–9.
20. Harel M, Ortenberg R, Varanasi SK, Mangalharra KC, Mardamshina M, Markovits E, et al. Proteomics of melanoma response to immunotherapy reveals mitochondrial dependence. *Cell* 2019;179:236–50.
21. Besser MJ, Shapira-Frommer R, Treves AJ, Zippel D, Itzhaki O, Schallmach E, et al. Minimally cultured or selected autologous tumor-infiltrating lymphocytes after a lympho-depleting chemotherapy regimen in metastatic melanoma patients. *J Immunother* 2009;32:415–23.
22. Greenberg E, Hershkovitz L, Itzhaki O, Hajdu S, Nemlich Y, Ortenberg R, et al. Regulation of cancer aggressive features in melanoma cells by MicroRNAs. *PLoS One* 2011;6:e18936.
23. Baruch EN, Ortenberg R, Avivi C, Anafi L, Dick-Necula D, Stossel C, et al. Immune coculture cell microarray—a feasible tool for high-throughput functional investigation of lymphocyte–cancer interactions. *Oncoimmunology* 2020;9:1741267.
24. Bates D, Mächler M, Bolker BM, Walker SC. Fitting linear mixed-effects models using lme4. *J Stat Softw* 2015;67.
25. Gu Z, Eils R, Schlesner M. Complex heatmaps reveal patterns and correlations in multidimensional genomic data. *Bioinformatics* 2016;32:2847–9.
26. Akbani R, Akdemir KC, Aksoy BA, Albert M, Ally A, Amin SB, et al. Genomic classification of cutaneous melanoma. *Cell* 2015;161:1681–96.
27. Quintás-Cardama A, Vaddi K, Liu P, Manshoury T, Li J, Scherle PA, et al. Preclinical characterization of the selective JAK1/2 inhibitor INCB018424: Therapeutic implications for the treatment of myeloproliferative neoplasms. *Blood* 2010;115:3109–17.
28. Shin DS, Zaretsky JM, Escuin-Ordinas H, Garcia-Diaz A, Hu-Lieskovan S, Kalbasi A, et al. Primary resistance to PD-1 blockade mediated by JAK1/2 mutations. *Cancer Discov* 2017;7:188–201.
29. Ishizuka JJ, Manguso RT, Cheruiyot CK, Bi K, Panda A, Iracheta-Velva A, et al. Loss of ADAR1 in tumors overcomes resistance to immune checkpoint blockade. *Nature* 2019;565:43–8.
30. Mueller A, Strange PG. The chemokine receptor, CCR5. *Int J Biochem Cell Biol* 2004;36:35–8.
31. Chen Y, Wang X. miRDB: an online database for prediction of functional microRNA targets. *Nucleic Acids Res* 2020;48:D127.
32. Van Damme H, Dombrecht B, Kiss M, Roose H, Allen E, Van Overmeire E, et al. Therapeutic depletion of CCR8+ tumor-infiltrating regulatory T cells elicits antitumor immunity and synergizes with anti-PD-1 therapy. *J Immunother Cancer* 2021;9:e001749.
33. Bonaventura P, Shekarian T, Alcazer V, Valladeau-Guilemond J, Valsesia-Wittmann S, Amigorena S, et al. Cold tumors: a therapeutic challenge for immunotherapy. *Front Immunol* 2019;10:168.
34. Kluger HM, Zito CR, Barr ML, Baine MK, Chiang VLS, Szoln M, et al. Characterization of PD-L1 expression and associated T-cell infiltrates in metastatic melanoma samples from variable anatomic sites. *Clin Cancer Res* 2015;21:3052–60.
35. Madore J, Vilain RE, Menzies AM, Kakavand H, Wilmott JS, Hyman J, et al. PD-L1 expression in melanoma shows marked heterogeneity within and between patients: Implications for anti-PD-1/PD-L1 clinical trials. *Pigment Cell Melanoma Res* 2015;28:245–53.
36. Alavi S, Stewart AJ, Kefford RF, Lim SY, Shklovskaya E, Rizos H. Interferon signaling is frequently downregulated in melanoma. *Front Immunol* 2018;9:1414.
37. Karachaliou N, Gonzalez-Cao M, Crespo G, Drozdowskyj A, Aldeguer E, Gimenez-Capitan A, et al. Interferon gamma, an important marker of response to immune checkpoint blockade in non-small cell lung cancer and melanoma patients. *Ther Adv Med Oncol* 2018;10:1758834017749748.
38. Nemlich Y, Baruch EN, Besser MJ, Shoshan E, Bar-Elm M, Anafi L, et al. ADAR1-mediated regulation of melanoma invasion. *Nat Commun* 2018;9:1–13.
39. Shoshan E, Mobley AK, Brauer RR, Kamiya T, Huang L, Vasquez ME, et al. Reduced adenosine-to-inosine miR-455-5p editing promotes melanoma growth and metastasis. *Nat Cell Biol* 2015;17:311–21.
40. Eisenberg E, Nemzer S, Kinar Y, Sorek R, Rechavi G, Levanon EY. Is abundant A-to-I RNA editing primate-specific? *Trends Genet* 2005;21:77–81.
41. Harlin H, Meng Y, Peterson AC, Zha Y, Tretiakova M, Slingluff C, et al. Chemokine expression in melanoma metastases associated with CD8+ T-cell recruitment. *Cancer Res* 2009;69:3077–85.
42. Hamid O, Robert C, Daud A, Hodi FS, Hwu W-J, Kefford R, et al. Safety and tumor responses with lambrolizumab (anti-PD-1) in melanoma. *N Engl J Med* 2013;369:134–44.
43. Song B, Shiromoto Y, Minakuchi M, Nishikura K. The role of RNA editing enzyme ADAR1 in human disease. *Wiley Interdiscip Rev RNA* 2022;13:e1665.
44. Fritzell K, XL Di, Lagergren J, Öhman M. ADARs and editing: The role of A-to-I RNA modification in cancer progression. *Semin Cell Dev Biol* 2018;79:123–30.
45. Gannon HS, Zou T, Kiessling MK, Gao GF, Cai D, Choi PS, et al. Identification of ADAR1 adenosine deaminase dependency in a subset of cancer cells. *Nat Commun* 2018;9:5450.
46. Wu Z, Zhou J, Zhang X, Zhang Z, Xie Y, LJ bin, et al. Reprogramming of the esophageal squamous carcinoma epigenome by SOX2 promotes ADAR1 dependence. *Nat Genet* 2021;53:881–94.